

# Upper Limit on the $\eta \rightarrow \gamma\gamma\gamma$ Branching Ratio with the KLOE Detector

The KLOE Collaboration

A. Aloisio<sup>g</sup>, F. Ambrosino<sup>g</sup>, A. Antonelli<sup>c</sup>, M. Antonelli<sup>c</sup>,  
C. Bacci<sup>m</sup>, G. Bencivenni<sup>c</sup>, S. Bertolucci<sup>c</sup>, C. Bini<sup>k</sup>,  
C. Bloise<sup>c</sup>, V. Bocci<sup>k</sup>, F. Bossi<sup>c</sup>, P. Branchini<sup>m</sup>,  
S. A. Bulychjov<sup>f</sup>, R. Caloi<sup>k</sup>, P. Campana<sup>c</sup>, G. Capon<sup>c</sup>,  
T. Capussela<sup>g</sup>, G. Carboni<sup>l</sup>, F. Ceradini<sup>m</sup>, F. Cervelli<sup>i</sup>,  
F. Cevenini<sup>g</sup>, G. Chiefari<sup>g</sup>, P. Ciambrone<sup>c</sup>, S. Conetti<sup>o</sup>,  
E. De Lucia<sup>k</sup>, P. De Simone<sup>c</sup>, G. De Zorzi<sup>k</sup>, S. Dell’Agnello<sup>c</sup>,  
A. Denig<sup>d</sup>, A. Di Domenico<sup>k</sup>, C. Di Donato<sup>g</sup>, S. Di Falco<sup>i</sup>,  
B. Di Micco<sup>m1</sup>, A. Doria<sup>g</sup>, M. Dreucci<sup>c</sup>, O. Erriquez<sup>a</sup>,  
A. Farilla<sup>m</sup>, G. Felici<sup>c</sup>, A. Ferrari<sup>m</sup>, M. L. Ferrer<sup>c</sup>,  
G. Finocchiaro<sup>c</sup>, C. Forti<sup>c</sup>, P. Franzini<sup>k</sup>, C. Gatti<sup>k</sup>, P. Gauzzi<sup>k</sup>,  
S. Giovannella<sup>c</sup>, E. Gorini<sup>e</sup>, E. Graziani<sup>m</sup>, M. Incagli<sup>i</sup>,  
W. Kluge<sup>d</sup>, V. Kulikov<sup>f</sup>, F. Lacava<sup>k</sup>, G. Lanfranchi<sup>c</sup>,  
J. Lee-Franzini<sup>c,n</sup>, D. Leone<sup>k</sup>, F. Lu<sup>c,b</sup>, M. Martemianov<sup>c</sup>,  
M. Matsyuk<sup>c</sup>, W. Mei<sup>c</sup>, L. Merola<sup>g</sup>, R. Messi<sup>l</sup>, S. Miscetti<sup>c</sup>,  
M. Moulson<sup>c</sup>, S. Müller<sup>d</sup>, F. Murtas<sup>c</sup>, M. Napolitano<sup>g</sup>,  
F. Nguyen<sup>m</sup>, M. Palutan<sup>c</sup>, E. Pasqualucci<sup>k</sup>, L. Passalacqua<sup>c</sup>,  
A. Passeri<sup>m</sup>, V. Patera<sup>c,j</sup>, F. Perfetto<sup>g</sup>, E. Petrolo<sup>k</sup>,  
L. Pontecorvo<sup>k</sup>, M. Primavera<sup>e</sup>, P. Santangelo<sup>c</sup>, E. Santovetti<sup>l</sup>,  
G. Saracino<sup>g</sup>, R. D. Schamberger<sup>n</sup>, B. Sciascia<sup>c</sup>, A. Sciubba<sup>c,j</sup>,  
F. Scuri<sup>i</sup>, I. Sfiligoi<sup>c</sup>, A. Sibidanov<sup>c,h</sup>, T. Spadaro<sup>c</sup>, E. Spiriti<sup>m</sup>,  
M. Testa<sup>k</sup>, L. Tortora<sup>m</sup>, P. Valente<sup>c</sup>, B. Valeriani<sup>d</sup>,  
G. Venanzoni<sup>i</sup>, S. Veneziano<sup>k</sup>, A. Ventura<sup>e</sup>, S. Ventura<sup>k</sup>,  
R. Versaci<sup>m</sup>, I. Vilella<sup>g</sup>, G. Xu<sup>c,b</sup>

<sup>1</sup> Corresponding author: B. Di Micco, Università “Roma Tre”, Via della Vasca Navale, 84, I-00146, Roma, Italy, e-mail dimicco@fis.uniroma3.it

- <sup>a</sup>*Dipartimento di Fisica dell'Università e Sezione INFN, Bari, Italy.*
- <sup>b</sup>*Permanent address: Institute of High Energy Physics, CAS, Beijing, China.*
- <sup>c</sup>*Laboratori Nazionali di Frascati dell'INFN, Frascati, Italy.*
- <sup>d</sup>*Institut für Experimentelle Kernphysik, Universität Karlsruhe, Germany.*
- <sup>e</sup>*Dipartimento di Fisica dell'Università e Sezione INFN, Lecce, Italy.*
- <sup>f</sup>*Permanent address: Institute for Theoretical and Experimental Physics, Moscow, Russia.*
- <sup>g</sup>*Dipartimento di Scienze Fisiche dell'Università "Federico II" e Sezione INFN, Napoli, Italy*
- <sup>h</sup>*Permanent address: Budker Institute of Nuclear Physics, Novosibirsk, Russia*
- <sup>i</sup>*Dipartimento di Fisica dell'Università e Sezione INFN, Pisa, Italy.*
- <sup>j</sup>*Dipartimento di Energetica dell'Università "La Sapienza", Roma, Italy.*
- <sup>k</sup>*Dipartimento di Fisica dell'Università "La Sapienza" e Sezione INFN, Roma, Italy.*
- <sup>l</sup>*Dipartimento di Fisica dell'Università "Tor Vergata" e Sezione INFN, Roma, Italy.*
- <sup>m</sup>*Dipartimento di Fisica dell'Università "Roma Tre" e Sezione INFN, Roma, Italy.*
- <sup>n</sup>*Physics Department, State University of New York at Stony Brook, USA.*
- <sup>o</sup>*Physics Department, University of Virginia, USA.*

---

## Abstract

We have searched for the  $C$ -violating decay  $\eta \rightarrow \gamma\gamma\gamma$  in a sample of  $\sim 18$  million  $\eta$  mesons produced in  $\phi \rightarrow \eta\gamma$  decays, collected with the KLOE detector at the Frascati  $\phi$ -factory DAΦNE. No signal is observed and we obtain the upper limit  $BR(\eta \rightarrow \gamma\gamma\gamma) \leq 1.6 \times 10^{-5}$  at 90% CL.

---

The decay  $\eta \rightarrow \gamma\gamma\gamma$  is forbidden by charge-conjugation invariance, if the weak interaction is ignored. The present limit for the  $\eta \rightarrow 3\gamma$  branching ratio,  $BR(\eta \rightarrow 3\gamma) \leq 5 \times 10^{-4}$  at 95% CL, is based on the result of the GAMS2000 experiment at Serpukhov [1], which studied neutral decays of  $\eta$  mesons from the reaction  $\pi^- p \rightarrow \eta n$  at a beam momentum of 30 GeV/c.

We have searched with KLOE for the decay  $\eta \rightarrow \gamma\gamma\gamma$  among four-photon events, corresponding to the two step process  $\phi \rightarrow \eta\gamma$ ,  $\eta \rightarrow \gamma\gamma\gamma$ . The KLOE detector [2–5], operates at the Frascati  $e^+e^-$  collider DAΦNE [6], which runs at a CM energy  $W$  equal to the  $\phi$ -meson mass,  $W \sim 1019.5$  MeV. Copious  $\eta$ -meson production is available from the decay  $\phi \rightarrow \eta\gamma$ , with a branching ratio of 1.3%. The highest  $\phi$ -production rate that has been obtained to date was  $\sim 240$   $\phi$ /s,

corresponding to  $\sim 3.1 \eta/s$ , in October 2002. At DAΦNE, because of the beam-crossing angle,  $\phi$  mesons are produced with a small transverse momentum, 12.5 MeV/c, in the horizontal plane. The present analysis is based on data collected in the years 2001 and 2002 for an integrated luminosity of  $410 \text{ pb}^{-1}$ , corresponding to  $1.8 \times 10^7 \eta$  mesons produced.

The KLOE detector consists of a large cylindrical drift chamber [2], DC, surrounded by a lead/scintillating-fiber sampling calorimeter [3], EMC, both immersed in a solenoidal magnetic field of 0.52 T with the axis parallel to the beams. Two small calorimeters [4] are wrapped around the quadrupoles of the low- $\beta$  insertion to complete the detector hermeticity. The DC tracking volume extends from 28.5 to 190.5 cm in radius and is 330 cm long, centered around the interaction point. The DC momentum resolution for charged particles is  $\delta p_{\perp}/p_{\perp}=0.4\%$ . Vertices are reconstructed with an accuracy of 3 mm. The calorimeter is divided into a barrel and two endcaps, and covers 98% of the total solid angle. Photon energies and arrival times are measured with resolutions  $\sigma_E/E = 0.057/\sqrt{E} \text{ (GeV)}$  and  $\sigma_t = 54 \text{ ps}/\sqrt{E} \text{ (GeV)} \oplus 50 \text{ ps}$ , respectively. Photon-shower centroid positions are measured with an accuracy of  $\sigma = 1 \text{ cm}/\sqrt{E} \text{ (GeV)}$  along the fibers, and 1 cm in the transverse direction. A photon is defined as a cluster of energy deposits in the calorimeter elements that is not associated to a charged particle. We require the distance between the cluster centroid and the nearest entry point of extrapolated tracks be greater than  $3 \times \sigma(z, \phi)$ .

The trigger [5] uses information from both the calorimeter and the drift chamber. The EMC trigger requires two local energy deposits above threshold ( $E > 50 \text{ MeV}$  in the barrel,  $E > 150 \text{ MeV}$  in the endcaps). Recognition and rejection of cosmic-ray events is also performed at the trigger level by checking for the presence of two energy deposits above 30 MeV in the outermost calorimeter planes. The DC trigger is based on the multiplicity and topology of the hits in the drift cells. The trigger has a large time spread with respect to the time distance between consecutive beam crossings. It is however synchronized with the machine radio frequency divided by four,  $T_{\text{sync}}=10.85 \text{ ns}$ , with an accuracy of 50 ps. For the 2001-2002 data taking, the bunch crossing period was  $T=5.43 \text{ ns}$ . The time ( $T_0$ ) of the bunch crossing producing an event is determined offline during event reconstruction.

The sensitivity of the search for  $\eta \rightarrow \gamma\gamma\gamma$  in KLOE is largely dominated by the ability to reject background. The dominant process producing four photons is  $e^+e^- \rightarrow \omega\gamma$ , due to initial-state radiation of a hard photon, followed by  $\omega \rightarrow \pi^0(\rightarrow 2\gamma)\gamma$ . Other processes with neutral secondaries only are also relevant. They can mimic four-photon events because of the loss of photons, addition of photons from machine background, or photon shower splitting. All the above effects are very difficult to reproduce accurately with Monte Carlo (MC) simulation. We therefore base our background estimates on data, and

use the MC only to evaluate the efficiency. An  $\eta \rightarrow 3\gamma$  generator using phase space for the internal variable distribution in the three-body decay has been used to produce 120,000  $\phi \rightarrow \gamma\eta$ ,  $\eta \rightarrow 3\gamma$  events.

For the analysis, only events without charged particle tracks are considered. The central value of the position of the beam-interaction point (IP), the CM energy, and the transverse momentum of the  $\phi$  are obtained run by run from large samples of Bhabha scattering events. The following requirements have been used to isolate  $\phi \rightarrow 4\gamma$  candidates:

- (1) The four photons must have
  - reconstructed velocity consistent with the speed of light,  $|t - r/c| < 5\sigma_t$ , where  $r$  is the distance traveled,  $t$  is the time of flight and  $\sigma_t$  is the time resolution;
  - photon energy  $E_\gamma > 50$  MeV;
  - photon polar angle  $\theta > 24.5^\circ$ .
- (2) The total energy and momentum of the four prompt photons must satisfy  $\sum_i E_i > 800$  MeV and  $|\sum_i \vec{p}_i| < 200$  MeV/c;
- (3) The opening angle between any photon pair must satisfy  $\theta_{\gamma\gamma} > 15^\circ$ .

83,906 events pass the cuts above. A kinematic fit is used to improve the energy-momentum resolution. The input variables  $x_i$  of the fit are

- the coordinates of the photon clusters in the calorimeter;
- the energies of the clusters;
- the times of flight of the photons;
- the coordinates of the  $e^+e^-$  interaction point;
- the energy and momentum of the  $\phi$  meson.

We minimize the  $\chi^2$  function

$$\chi^2 = \sum_i \frac{(x_i - \mu_i)^2}{\sigma_i^2} + \sum_j \lambda_j F_j(\mu_k),$$

where  $F_j(\mu_k)$  are the energy, momentum, and time constraints and  $\lambda_i$  are Lagrangian multipliers. The  $\chi^2$  value of the fit is used to reject background. Events with  $\chi^2 < 25$  are retained, the number of degrees of freedom being 8.

After this cut we are left with 52577 events. The residual background after the cut is due to events with neutral pions (fig. 1, left), coming mainly from  $e^+e^- \rightarrow \omega\gamma$  with  $\omega \rightarrow \pi^0\gamma$ . This can be seen in fig. 1, right, where the invariant mass of the  $\pi^0$  and the highest energy photon, in the  $\pi^0\gamma\gamma$  hypothesis,  $\gamma_{\text{hi}}$ , shows a clear peak at the  $\omega$  mass. Other background sources with a  $\pi^0$  in the final state are the decays  $\phi \rightarrow \pi^0\gamma$ ,  $\phi \rightarrow f_0\gamma \rightarrow \pi^0\pi^0\gamma$ , and  $\phi \rightarrow a_0\gamma \rightarrow \eta\pi^0\gamma$ . We reject the main part of these events by a cut on the invariant mass of any photon pairs:  $90 < m(\gamma\gamma) < 180$  MeV.

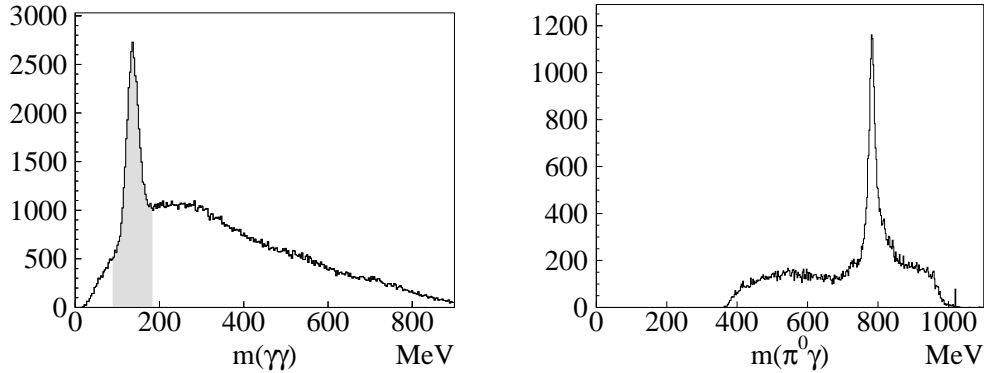


Fig. 1. Distribution of the invariant masses  $m(\gamma\gamma)$  computed for all photon pairs, left and  $m(\pi^0\gamma_{\text{hi}})$ , right. The shaded interval is removed before further analysis.

8,268 events survive the cuts. In the decay  $\phi \rightarrow \eta\gamma$ , the energy of the recoil photon in the CM of the  $\phi$  is 363 MeV. In the complete chain  $\phi \rightarrow \eta\gamma$ ,  $\eta \rightarrow 3\gamma$ , 363 MeV is also the most probable energy of the most energetic photon,  $\gamma_{\text{hi}}$ . Fig. 2, left, shows an MC simulation of the  $\gamma_{\text{hi}}$  energy spectrum for the signal. Fig. 2, right, shows the  $E(\gamma_{\text{hi}})$  distribution for the data sample. No peak is observed around 363 MeV. To evaluate an upper limit on the number of

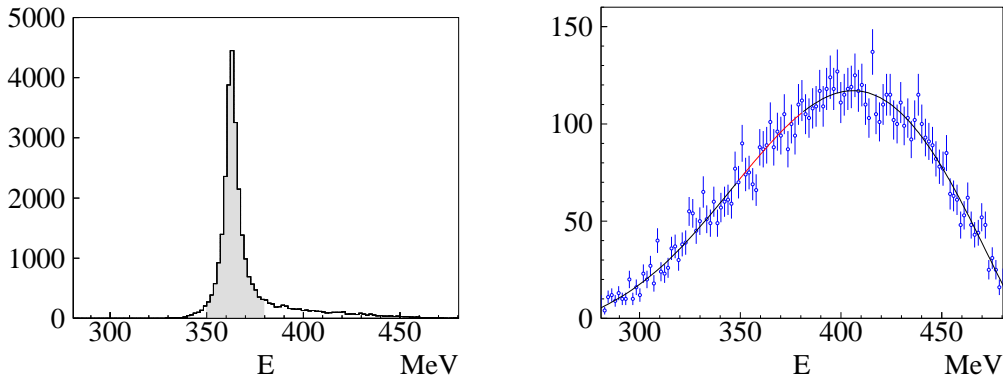


Fig. 2. Distribution of the energy  $E(\gamma_{\text{hi}})$ , in the  $\phi$  CM, for the MC simulated signal (left) and for the data (right). See text for discussion of the background fit.

$\eta \rightarrow 3\gamma$  events, we choose as the signal region the interval  $350 < E(\gamma_{\text{hi}}) < 379.75$  MeV (17 bins, 1.75-MeV wide). We estimate the background by fitting the  $E(\gamma_{\text{hi}})$  distribution on both sides of the expected signal region, in the intervals  $280 < E < 350$  and  $379.75 < E < 481.25$  MeV. We fit the background using 3<sup>rd</sup> to 6<sup>th</sup> order polynomials. The 5<sup>th</sup> order polynomial shown in fig. 2 gives the best fit, with  $\chi^2/\text{dof} = 78/92 = 0.85$ . We use the result to obtain the expected number of background events in each bin,  $N_i^b$ . The total number of observed events in the signal window is 1513 while from integration of the polynomial we obtain 1518 events in the same region.

The upper limits have been evaluated using Neyman's construction procedure

[7]. To evaluate the agreement with the background distribution in the signal region, we use

$$F = \sum_i \frac{(N_i - N_i^b)^2}{N_i^b},$$

where  $N_i$  is the number of observed counts in the  $i^{\text{th}}$  bin, and the sum is over bins in the signal region. We obtain the distribution function for  $F$  for various values of the number of signal counts  $s$  as follows. First, we *construct* the values  $N_i$  by sampling a Poisson distribution with mean  $\langle N_i(s) \rangle = N_i^b + s \times f_i$ , where  $f_i$  is the fraction of signal events (fig. 2, left) in the  $i^{\text{th}}$  bin, and evaluate  $F$ . Repeating this procedure  $10^6$  times for each value of  $s$  then gives the complete p.d.f., which is numerically integrated to obtain the 90% and 95% contours in Neyman's construction. We then evaluate  $F$  using the *observed*  $N_i$ . We find  $F = 13.45$ , from which we obtain

$$N_{\eta \rightarrow 3\gamma} \leq 63.1 \text{ at } 90\% \text{ CL}; \leq 80.8 \text{ at } 95\% \text{ CL}.$$

To convert this result into an upper limit for the branching ratio, we normalize to the number of  $\eta \rightarrow 3\pi^0$  events [8] found in the same data sample,  $N(\eta \rightarrow 3\pi^0) = 2,431,917$ . The efficiencies are  $\epsilon(\eta \rightarrow 3\pi^0) = 0.378 \pm 0.008(\text{syst.}) \pm 0.001(\text{stat.})$  and  $\epsilon(\eta \rightarrow 3\gamma) = 0.200 \pm 0.001(\text{stat.}) \pm 0.002(\text{syst.}) \pm 0.006(\chi_{\text{cut}}^2)$ . The systematic error includes residual uncertainties on the photon detection efficiency [9]. For the ratio of the two branching ratios we obtain

$$\frac{\text{BR}(\eta \rightarrow 3\gamma)}{\text{BR}(\eta \rightarrow 3\pi^0)} = \frac{N_{\eta \rightarrow 3\gamma} \epsilon_{\eta \rightarrow 3\pi^0}}{N_{\eta \rightarrow 3\pi^0} \epsilon_{\eta \rightarrow 3\gamma}} \leq 4.9 \times 10^{-5} \text{ } 90\% \text{ CL},$$

$$\leq 6.3 \times 10^{-5} \text{ } 95\% \text{ CL}.$$

Using the value  $\text{BR}(\eta \rightarrow 3\pi^0) = (32.51 \pm 0.29)\%$  [10], we derive the upper limit

$$\text{BR}(\eta \rightarrow 3\gamma) \leq 1.6 \times 10^{-5} \text{ at } 90\% \text{ CL} \quad \text{and} \quad \leq 2.0 \times 10^{-5} \text{ at } 95\% \text{ CL}.$$

The efficiency quoted above for  $\eta \rightarrow 3\gamma$ , which depends on the cut  $\chi^2 < 25$  applied after the kinematic fit of all four-photon events, is evaluated by MC simulation. We check the validity of the MC result by comparison with the  $\chi^2$  distribution for radiative events  $e^+e^- \rightarrow \gamma\omega \rightarrow \gamma\gamma\pi^0 \rightarrow 4\gamma$ . A sample of these events is selected from among all four-photon candidates by requiring  $128 < m(\gamma\gamma) < 145$  MeV for the neutral pion and  $760 < m(\pi^0\gamma) < 815$  MeV for the  $\omega$ . The fraction of these events with  $\chi^2 < 25$  after the kinematic fit differs from the MC estimate by  $\sim 3\%$ . This value is included in the quoted error for  $\epsilon(\eta \rightarrow 3\gamma)$ .

To check whether the kinematic fit introduces a bias in the energy distribution of the signal photons, we have analyzed a sample of  $\phi \rightarrow \eta\gamma_{\text{rec}} \rightarrow \gamma\gamma\gamma_{\text{rec}}$  events, in which the energy of the recoil photon is the same as in the case of

interest. Fig. 3 shows the energy distribution of the photons as obtained after the kinematic fit for data and MC events. The two distributions are in good agreement within errors.

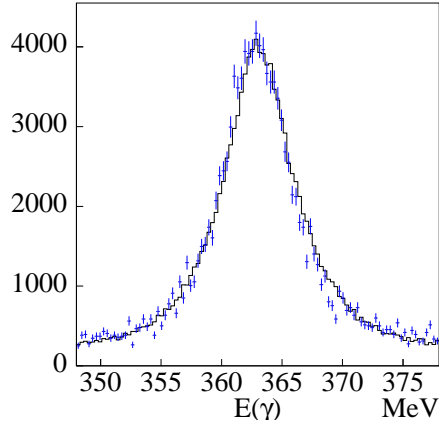


Fig. 3. Distribution of  $E(\gamma)$  for the  $\phi \rightarrow \eta\gamma\gamma \rightarrow (\gamma\gamma)\gamma$  event sample for the data (points) and MC simulated events (continuous histogram).

The stability of the upper limit versus the background estimate has been checked by comparing the results of polynomials of different degree for fitting the  $E(\gamma_{hi})$  distribution outside the signal region. A 3<sup>rd</sup> order polynomial doesn't describe the background shape well. A 4<sup>th</sup> order polynomial gives a lower value for the signal yield, while a 6<sup>th</sup> order polynomial gives the same result. We have also checked the stability of the result by changing the window chosen for evaluation of the upper limit obtaining a maximum variation of 11%. We have also evaluated the  $\eta \rightarrow 3\gamma$  acceptance using the matrix element of ref.[12] and we find a value 5% lower. Therefore systematic effects can be summarized: background estimation and window variation 11%,  $\epsilon(\eta \rightarrow 3\pi^0)/\epsilon(\eta \rightarrow 3\gamma)$  1%,  $\chi^2$  cut 3%, decay model 5%. We thus feel confident about the procedure adopted. Our limit

$$\text{BR}(\eta \rightarrow \gamma\gamma\gamma) \leq 1.6 \times 10^{-5} \text{ at 90\% CL or } \leq 2.0 \times 10^{-5} \text{ at 95\% CL}$$

is the strongest limit at present against possible violation of charge-conjugation invariance in the decay  $\eta \rightarrow 3\gamma$ .<sup>2</sup> An estimate for  $\Gamma(\eta \rightarrow 3\gamma)$ , including contributions from weak interactions, is given in Ref. 11. Using the estimate for  $\pi^0 \rightarrow 3\gamma$  [12], one finds  $\text{BR}(\eta \rightarrow 3\gamma) < 10^{-12}$ , which is quite a long way from the result above. The absence of the decay  $\eta \rightarrow 3\gamma$  therefore confirms the validity of charge-conjugation invariance in strong and electromagnetic interactions.

We thank the DAΦNE team for their efforts in maintaining low background

<sup>2</sup> A preliminary unpublished 2002 result by the Crystal Ball,  $\text{BR}(\eta \rightarrow 3\gamma) \leq 1.8 \times 10^{-5}$  at 90% CL, is mentioned in [13].



running conditions and their collaboration during all data taking. We want to thank our technical staff: G.F. Fortugno for his dedicated work to ensure efficient operations of the KLOE Computing Center; M. Anelli for his continuous support of the gas system and detector safety; A. Balla, M. Gatta, G. Corradi and G. Papalino for electronics maintenance; M. Santoni, G. Paoluzzi and R. Rosellini for general support of the detector; C. Pinto (Bari), C. Pinto (Lecce), C. Piscitelli and A. Rossi for their help during major maintenance periods. This work was supported in part by DOE grant DE-FG-02-97ER41027; by EU-RODAPHNE, contract FMRX-CT98-0169; by the German Federal Ministry of Education and Research (BMBF) contract 06-KA-957; by Graduiertenkolleg ‘H.E. Phys. and Part. Astrophys.’ of Deutsche Forschungsgemeinschaft, Contract No. GK 742; by INTAS, contracts 96-624, 99-37; and by TARI, contract HPRI-CT-1999-00088.

## References

- [1] D. M. Alde et al., *Z. Phys.* C25 (1984) 225
- [2] KLOE Coll., M. Adinolfi et al., *Nucl. Instrum. Meth.* A488 (2002) 51.
- [3] KLOE Coll., M. Adinolfi et al., *Nucl. Instrum. Meth.* A482 (2002) 363.
- [4] KLOE Coll., M. Adinolfi et al., *Nucl. Instrum. Meth.* A483 (2002) 649.
- [5] KLOE Coll., M. Adinolfi et al., *Nucl. Instrum. Meth.* A492 (2002) 134.
- [6] S. Guiducci, *Proc. of the 2001 Particle Accelerator Conf.*, P. Lucas, S. Webber (Eds.), Chicago, IL, U.S.A. (2001)
- [7] G.J. Feldman, R.D. Cousins, *Phys. Rev.* D57 (1998) 3873; J. Neyman, *Phil. Trans.* A236 (1937) 333
- [8] S. Giovannella and S. Miscetti, *Phi cross section measurement*, KLOE note n. 177 (2002), URL: <http://www.lnf.infn.it/kloe/documents.html>.
- [9] M. Palutan, T. Spadaro and P. Valente, *Measurement of  $\Gamma(K_S \rightarrow \pi^+\pi^-)/\Gamma(K_S \rightarrow \pi^0\pi^0)$  with KLOE 2000 data*, KLOE note n. 174, (2002).
- [10] K. Hagiwara et al., *Phys. Rev.* D66 (2002) 010001
- [11] P. Herczeg, *Proc. Int. Workshop on Production and Decay of Light Mesons*, P. Fleury ed., Paris, France, (World Scientific, 1988), 16.
- [12] D.A. Dicus, *Phys. Rev.* D12 (1975) 2133
- [13] B.M.K. Nefkens and J.W. Price, *Phys. Scripta*, T99 (2002) 114